Building an experimental model of the human body with non-physiological parameters

Joseph M. Labuz[1,2], **Christopher Moraes**[3], **David R. Mertz**[1,2], **Brendan M. Leung**[4,5], and **Shuichi Takayama**[1,2,6,7]

[1]Department of Biomedical Engineering, College of Engineering and School of Medicine, University of Michigan, 2200 Bonisteel Blvd, Ann Arbor, MI 48109, USA

[2]Biointerfaces Institute, University of Michigan, 2800 Plymouth Road, North Campus Research Complex (NCRC), MI 48109, USA

[3]Department of Chemical Engineering, Faculty of Engineering, McGill University, 3610 University Street, Montreal, QC, H3A 0C5, Canada

[4]Department of Applied Oral Sciences, Faculty of Dentistry, Dalhousie University, 5981 University Ave, Halifax, Nova Scotia (NS), B3H 4R2, Canada

[5]School of Biomedical Engineering, Faculties of Medicine and Engineering, Dalhousie University, 5981 University Ave, Halifax, Nova Scotia (NS), B3H 4R2, Canada

[6]Macromolecular Science and Engineering Center, College of Engineering, University of Michigan, 2300 Hayward St., Ann Arbor, MI 48109, USA

[7]Michigan Center for Integrative Research in Critical Care, University of Michigan, Ann Arbor, MI 48109, USA

Abstract

New advances in engineering and biomedical technology have enabled recent efforts to capture essential aspects of human physiology in microscale, *in-vitro* systems. The application of these advances to experimentally model complex processes in an integrated platform — commonly called a 'human-on-a-chip (HOC)' — requires that relevant compartments and parameters be sized correctly relative to each other and to the system as a whole. Empirical observation, theoretical treatments of resource distribution systems and natural experiments can all be used to inform rational design of such a system, but technical and fundamental challenges (e.g. small system blood volumes and context-dependent cell metabolism, respectively) pose substantial, unaddressed obstacles. Here, we put forth two fundamental principles for HOC design: inducing *in-vivo*-like cellular metabolic rates is necessary and may be accomplished *in-vitro* by limiting O_2 availability and that the effects of increased blood volumes on drug concentration can be mitigated through pharmacokinetics-based treatments of solute distribution. Combining these principles with natural observation and engineering workarounds, we derive a complete set of design criteria for a practically realizable, physiologically faithful, five-organ millionth-scale ($\times 10^{-6}$) microfluidic model of the human body.

Correspondence should be addressed to S.T. (takayama@umich.edu).

0. INNOVATION

An integrated experimental model of the human body (a "human-on-a-chip" or HOC) holds great promise for drug discovery, personalized medicine and basic research. Despite recent achievements in this field, substantial challenges remain in faithfully recapitulating macro human function at a micro scale. Breaking with convention, we propose that non-physiologic design parameters (e.g. low "blood" oxygen carrying capacity) can be employed to induce *in-vivo*-like HOC behavior. We apply this strategy — supported by experimental and theoretical evidence — to provide detailed design criteria for a five-organ HOC capable of matching macro human function across key criteria.

1. INTRODUCTION

Advances in micro-scale engineering, cell sourcing and culture techniques are presenting new opportunities to recapitulate key structural and functional characteristics of the human body in controlled, *in-vitro*, experimental systems. Already, organ-level devices (commonly called 'organs-on-a-chip') are quite prolific[1–3]. Efforts at devising systems-level platforms (i.e. HOCs) hold even greater promise[4–7]. Ideally, these small HOCs would predict the effects of potential drugs or toxins on the human body[8–10], significantly reducing costs associated with animal and human clinical trials in the drug discovery pipeline, clarifying mechanisms of human health and disease and introducing new opportunities in personalized medicine. However, unresolved issues in both the design and fabrication of such systems present scientists and engineers with a complex, interdependent set of problems.

Animal basal metabolic rate (BMR) has been shown to scale with animal mass raised to some power[11]. Although there remains some debate as to the exact value of the exponent[12], recent research has focused on how nutrient distribution networks generally control the relationship between organism size and metabolism[13,14]. Thus, many important physical parameters scale with organism mass (M) raised to the power of a multiple of ¼ (e.g. metabolic rate, $M^{3/4}$; heart rate, $M^{-1/4}$; and blood volume, M^1), called quarter-power scaling relationships (QPSRs). These QPSRs[6,15,16], along with order of magnitude estimates[17,18], residence time and physiologically based pharmacokinetic/pharmacodynamic (PB-PKPD) models[4,5,8,19–21], empirical allometry[22,23] and functional approaches[22–24] have all been used in the design of HOCs. Although these approaches do inform values for organ compartment size and other physiological parameters, they also present two classes of intractable problems in the design and construction of such systems. The first type of problem is purely technical in nature (e.g. the need for microfluidic systems of low circulating fluid volume, but sufficient tissue volume) and may eventually be solved by steady improvement in techniques and capabilities[2,7,18,21,22]. Fundamental problems (e.g. the context-dependent change in cellular BMR), however, can only be addressed by a thoughtful and deliberate design strategy[25–28].

We propose that these challenges themselves only merit concern so far as they affect the end output of the HOC. That is, the *structure* of a $\times 10^{-6}$ HOC may assume strange and unexpected forms so long as the *function* — the cellular- and system-level behavior of the HOC — is accurate and relatable to human physiology. Therefore, discrete parts of an HOC need not necessarily be confined by conventional notions of what constitutes "normal" or "physiologic". To that end, we focus on designing a $\times 10^{-6}$ HOC capable of mimicking key *functions* of a macro human, specifically (1) cellular- and macro-scale BMRs and (2) basic pharmacokinetics. We further demonstrate how naturally-occurring biological systems may stray from structures of typical physiology (e.g. a hemoglobin-free vertebrate), yet produce species capable of adapting and surviving nonetheless. As modification of any particular system parameter necessarily affects all others, both natural and artificial design alterations demand a holistic approach. Applying these general principles, we propose specific design parameters for an HOC that is practical in terms of fluid-to-cell ratios and is a $\times 10^{-6}$ miniaturization of the human body with regard to total cell mass, yet remains a faithful model of macroscopic human physiology with regards to cellular BMR, basic pharmacokinetics and inter-organ scaling.

2. CONTROL OF CELLULAR BMR

As predicted by QPSRs, cellular metabolic rate scales with animal mass[25,26,28]. However, cells cultured *in-vitro* tend to operate at an elevated metabolic rate regardless of their organism of origin (Fig. 1a)[25,27]. Without accounting for this phenomenon, cells in an *in-vitro* HOC would have a high cellular BMR, more akin to cells in a mouse than in a human. Thus, the system BMR of the animal-on-a-chip diverges from that of the corresponding real animal; the magnitude of the error increases with animal size as $\propto M^{1/4}$ (Fig. 1b). For example, failure to consider the context-dependent behavior of cells in attempting to design a $\times 10^{-6}$ model of a human would result in an HOC wherein the cellular BMR is high and thus approximates that of a mouse and the system BMR is also high and approximates that of a $\times 10^{-6}$ elephant! Because of this non-linearity in scaling (i.e. M raised to a power $\neq 1$), rational design — and control — of the metabolic infrastructure of an HOC is crucial. We have previously proposed that designers must force cells in an HOC to function as they would in the macroscopic human body — that is, designers must suppress cellular BMR to match *in-vivo* levels outlined in Fig. 1a, in a strategy termed metabolically supported scaling[24].

Although others have demonstrated metabolic control by regulating glucose[29], ions[30], extracellular matrix (ECM) cues[31] and oxygen[24], we propose to limit O_2 availability *for the expressed purpose* of suppressing cellular BMR and inducing a more *in-vivo* like response from an HOC. Not only does this approach more closely approximate conditions in the body than the hyperoxic conditions of incubator cell culture, but *in-situ* microfluidic O_2 sensing and control is an established and active area of research[32–34]. To demonstrate that O_2 deprivation is a viable method for controlling cellular metabolic rate, we examine the behavior of human cell lines in atmospheric (20%) and physiotypic (7% and 2%) oxygen environments. Using AlamarBlue as an indicator of cellular respiration, we show that HepG2-C3A, HS-5, IMR-90 and HEK-293 cells all demonstrate significant ($p < 0.001$) oxygen conformance. A similar effect has been noted by measuring oxygen consumption

rather than AlamarBlue reduction as well as predicted numerically[35,36]. As oxygen decreases, cellular metabolism follows — at physiotypic oxygen tension, cellular respiration is reduced by nearly fivefold (Fig. 2). Importantly, in no cases did AlamarBlue metabolism drop to zero indicating that, even after four hours culture in each O_2 atmosphere, the cells remained viable. Total cellular BMR is likely to be slightly higher than these measured values since our AlamarBlue indicator fails to respond to the anaerobic ATP production which yields ~10× less energy than aerobic processes.

Although cellular BMR saw at most a fivefold reduction, compared to the 10× theoretical difference between cells *in-vivo* and *in-vitro* (Fig. 1a), these results demonstrate that oxygen deprivation is a viable strategy for reducing cellular BMR to be more in line with "natural" levels. Moreover, the results demonstrate that cells remained viable in pO_2 up to 10× lower than a conventional cell culture incubator (perhaps unsurprising given that such low O_2 levels are part of the *in-vivo* environment for most cells). While we do not claim that data implies a specific O_2 range for "optimal" cell function, it does, combined with existing theory, suggest a more "*in-vivo-like*" set of parameters than those used in conventional cell culture. While it is likely that other processes may be affected by this change in cell BMR (e.g. drug metabolism) that is precisely the point, as these changes are likely to *more* accurately reflect cell behavior in the body. Therefore, in contrast with suggested strategies to create a suitable oxygen-rich blood substitute for use in an HOC[22,23,37], we propose limiting oxygen availability to manipulate cellular BMR[24]. Combined with other O_2 sensing and control systems[32–34], we may achieve normoxic or (where necessary) hypoxic conditions *in-situ* to ensure that both cell- and system-level metabolic rates are appropriately scaled to those of a full-size human.

3. AN EXAMPLE OF EXTRA-PHYSIOLOGIC SURVIVAL: THE ICEFISH

The design modifications proposed in the previous section beg the question of whether such extreme departures from expected physiologic parameter values are acceptable. Would an organism with drastically altered blood O_2 carrying capacity or completely lacking hemoglobin be viable at all? Fortunately, Nature herself has provided a unique example of such extra-physiologic adaptation and survival. The family *Channichthyidae* (sometimes called 'icefish') comprises hemoglobin-negative (Hb−) fish living in the Antarctic waters of the Southern Ocean. First documented in the 1840s, initial attempts to examine the fish were thwarted by an uncooperative cat who absconded with the specimen before it could be further studied[38]. Subsequent investigations highlighted family members', including *Chaenocephalus aceratus*' (Fig. 3a), startling lack of blood pigment and hemoglobin (Fig. 3b)[39–42]. Just as technical and fundamental limitations force HOC designers to contort system parameters in strange or unexpected ways, so too has nature forced *C. aceratus* to counter its own maladaptation in order to survive.

To demonstrate, and perhaps learn from, this extra-physiologic survival, we examine the fish in more detail. As a control, we use a cousin of *C. aceratus*, *Notothenia coriiceps* (also called *neglecta*), from the common suborder *Notothenioidei*[43]. *N. coriiceps* shares a similar environment and metabolic rate (measured by oxygen consumption) as *C. aceratus*[44–46], but unlike the icefish, produces Hb at normal levels. Starting from a healthy *N. coriiceps*, we

remove Hb and then apply the adaptations that allow *C. aceratus* to thrive: increasing cardiac output by a factor of nearly two and allowing for increased cutaneous respiration[40,41,44–48]. The result is a test-fish with several surprising extra-physiologic features, but nevertheless capable of survival (Table 1 and Supplementary Information SI1.1). In particular, the ability of *C. aceratus* to absorb oxygen through its skin evokes polydimethylsiloxane (PDMS) — a common polymer in microfluidic and biomedical research applications that has similar properties of gas permeability (Supplementary Information S1.2).

In addition to larger-than-expected cardiac output, *C. aceratus* also has a blood volume of ~90 mL/kg, nearly twofold greater than the ~50 mL/kg expected for a fish its size[42,46,49–51]. Another member of *Channichthyidae*, *C. hamatus*, has a blood volume over twofold its predicted value[49]. These Hb– fish substantially exceed expected blood volumes yet thrive (Supplementary Information S1.3), reinforcing the idea that extra-normal physiology can be an acceptable mechanism to survive in the face of limitations. Related to that increased blood volume, *C. aceratus* also exhibits increased capillary density. Recent results demonstrated that three different metrics of vascularization were all ~twofold greater in C. aceratus than in *N. coriiceps* (Figs. 4a and 4b)[52]. Therefore, even though blood flow rates are double in *C. aceratus*, so too is organ blood volume, indicating that tissue residence times — a key parameter in PB-PKPD models — should also remain unchanged between it and *N. coriiceps*.

This increased vascularity also helps compensate for dilution of soluble factors (e.g. O_2, drugs or hormones) due to increased blood volume. At steady state the perfusion-limited diffusion of molecules from blood into tissue is described by Equation (1):

$$D \cdot \nabla^2 C = R, \quad (1)$$

where *C* is the concentration, *D* is the diffusion coefficient and *R* is the uptake of solute by cells, governed in this case by Michaelis–Menten kinetics[17,53]. Although a decrease in blood concentration leads to a decrease in potential gradient to drive diffusion, a corresponding decrease in intervessel distance (IVD) suggests that solute penetration may be similar, shown here specifically for O_2 (Fig. 4c; parameter values in Supplementary Information S1.4). This icefish adaptation is another example of nature finding a holistic, multi-faceted solution to physiologically challenging conditions. Of course, applying designs such as these to an HOC may still introduce problems with drugs or molecules that act in a concentration-dependent manner on the blood vessels themselves as well as other unforeseen consequences. Conversely, these data also suggest that depletion of soluble factors (e.g. oxygen) could be achieved over shorter distances, an important design consideration for engineering organ compartments such as the liver[17,54]. Nevertheless, this preliminary analysis demonstrates that blood O_2 carrying capacity and the presence of Hb may be tuned to counter maladaptations — or possibly induce more appropriate cellular metabolic behavior. The icefish further suggests that increased blood volumes may be accommodated without drastically altering organism pharmacokinetics or certain stromal solute concentration gradients.

4. A DISTRIBUTION-INFORMED APPROACH TO HOC BLOOD VOLUME

Designing an HOC according to QPSRs alone would result in a system blood volume of ~6 μL, too small for even cutting-edge microfluidics and an acknowledged problem in the field[7,18,21,22,24]. Although a 10× (or greater) increase would yield an HOC with a more manageable circulating volume, it would also dilute soluble factors and strain physiology to a much greater extent than the ~twofold increase in volume observed in *C. aceratus*. Therefore, we adopt a pharmacokinetic approach to investigate whether and to what extent the blood volume of an HOC can be increased while maintaining physiological relevance.

When a drug is administered, only a portion circulates dissolved in the blood. Accordingly, pharmacologists define volume of distribution, V_D, to describe how much drug is available in the plasma compared to the initial dose[55,56]. Conceptually, V_D closely resembles a partition coefficient describing the equilibrium distribution of a drug between the body and the blood. Using a slightly different approach, we consider the distribution of a drug between body water — including blood — and tissue. Therefore, this treatment is most applicable to small, perfusion-limited drugs without substantial serum protein binding. This ratio, K, is defined by Equation (2):

$$K = \frac{C_T}{C_W}, \quad (2)$$

where K is the partition or distribution coefficient, C_T is the concentration of drug in body tissue and C_W is the concentration of drug in body water. Ignoring excretion and metabolism and devolving the concentration terms to amount over volume,

$$K = \frac{\left(Dose - X_W\right) \big/ V_T}{X_W \big/ V_W}, \quad (3)$$

where *Dose* is the total amount of drug in the system, X_W is the amount of drug in the body water, V_T is the tissue volume and V_W is the volume of body water. Assuming no difference in concentration of drug in body water and concentration of drug in blood (C_B) and introducing V_O for non-blood body water volume (i.e. $V_W = V_B + V_O$), we rearrange to obtain Equation (5):

$$K + \frac{X_W \cdot V_W}{V_T \cdot X_W} = \frac{Dose}{V_T \cdot C_B}, \quad \text{and} \quad (4)$$

$$C_B = \frac{Dose}{(V_O + V_B) + K \cdot V_T}. \quad (5)$$

If we apply an arbitrary Z-fold increase to the blood volume compartment and normalize the result to the $Z = 1$ condition, C_{B0}, Equation (6) follows:

$$C_B \bigg/ C_{B0} = \frac{(V_o + V_B) + K \cdot V_T}{(V_o + Z \cdot V_B) + K \cdot V_T}. \quad (6)$$

In general, C_B falls as $1/Z$. However, the partitioning properties of the drug and the fact that V_B is a small fraction of the total system water volume serve to substantially temper the effect of increasing Z on blood concentration (Supplementary Information S2). For example, this treatment suggests that a highly hydrophilic drug, epinephrine, can tolerate ~10× increase in blood volume with only a ~twofold change in blood concentration. More hydrophobic drugs, such as amiodarone, are predicted to show almost no change in blood level at higher values of Z, and would require ~10^6 increase in blood volume to approach that same two-fold dilution.

To test these predictions, we construct a simple model of the body mimicking the two-compartment structure of our theoretical treatment. The water compartment, including variable blood volume, is represented by phosphate buffered saline and tissue is represented by an organic liquid (here, 1-octanol). The concentration of three small-molecule drugs — epinephrine, propranolol and amiodarone — was measured and normalized to the $Z = 1$ condition. The data (mean ± S.D.), along with curves representing the values predicted by Equation (6) are plotted in Fig. 5a. All three cases show reasonable agreement between predicted and experimental values. For scenarios where even these small dilutions are unacceptable, or in instances where the preceding treatment does not apply, other pharmacokinetic-based approaches may be useful, especially if PDMS or another gas-permeable material is used to decouple O_2 delivery from blood flow rate (Supplementary Information S3).

To illustrate this concept another way, we hold the aqueous phase constant, vary the mass presence of an organic depot (here represented by adipose spheroids instead of octanol) and assay for health of a HepG2 liver cell monolayer in the presence of differing concentrations of hydrophobic (amiodarone; $V_D = 4,260$ L for a 70-kg man) and hydrophilic (acetaminophen; $V_D = 66.5$ L) drugs. According to Equation (6), the high value of K for a hydrophobic compound amplifies the effects of increasing organic phase mass, leading to substantial protection of the HepG2 monolayer even at >10× the lethal concentration of amiodarone; the same changes in the face of increasing acetaminophen dosing shows no such effect (Fig. 5b). Combined with the theoretical treatment developed here for solutes of varying hydrophobicity in aqueous and organic phases of varying volume, these results demonstrate that HOC designers may be able to systematically predict the effects of

changing system fluid volumes and therefore compensate for such changes in their experimental design.

5. HOC DESIGN

5.1 Organ compartment design strategy

To design each organ compartment, we build on metabolically supported functional scaling (MSFS) strategies proposed previously, as well as other, similar, schemes[22,24,57]. The specific approach of Moraes *et al.* classifies organs according to principle function: two-dimensional (F-2D) or membranous tissue (e.g. lung) is scaled by surface area while functionally three-dimensional (F-3D) or lobular tissue (e.g. adipose) is scaled by volume[24]. Since this approach relies on principles of Euclidian geometry, it avoids inconsistencies that appear when empirical laws are extrapolated outside the range of the original dataset — a key problem for applying empirical, allometric organ–organism size relationships to HOC design[22,23]. Design parameters for F-2D organs are achieved by scaling according to surface area and compartment size is selected to match fluidic shear values found *in-vivo* for each tissue. F-3D organs are simply scaled by mass. For more complicated organs that may be classified as both F-2D and F-3D (e.g. liver), we used a two-compartment approach: one section with high surface area and another with high mass that together approach the appropriate values (Table 2). Spheroids and other tissue aggregation strategies may be particularly useful in these cases (Supplementary Information S4).

The endothelium presents another special case. Since several sources estimate the endothelial surface area of the body at 1,000 m^2 or greater[58–60], including the whole of the endothelium in this HOC would be an impossible undertaking. Since the endothelium mainly acts in concert with its associated organ rather than as a distinct entity, we include only endothelial tissue from organs already represented in this model (lung and liver). These tissues serve to recapitulate endothelial cell function within the organs included in this design and also provide a readout for general endothelial "health" across the HOC.

In addition to the organs *explicitly* included in this HOC design, we must also account for the body volume not represented by any of the designated organ compartments. Including a blank "other organs" zone to represent *implied* (but absent) organs ensures that our total system mass will be commensurate with that of a macro version and other groups have included "missing organ formulators" and "other tissues" compartments to similar ends[19,20,22,24]. Importantly, since we justify a substantially increased blood volume based in part on a volume distribution-based treatment that considers the entire body volume, it is critical that volume be faithfully replicated in our model system.

5.2 Overall design parameters

The insights provided by our examinations of metabolic scaling, *C. aceratus'* unique physiology, and volume of distribution considerations indicate that we need not be confined by preconceived notions of what is or is not "physiologic" in designing an HOC. Instead, it is the ultimate response — the function — of the HOC and not the underlying structure that is paramount. Specifically:

1. Without additional controls, on-chip cellular BMR will exceed *in-vivo* levels and cause a fundamental mismatch between the model system and reality. We propose limiting oxygen delivery as one effective mechanism for controlling cellular BMR.

2. Lack of Hb or an Hb substitute does not doom a vertebrate organism (or an HOC) *ex ante*. In fact, by introducing systemic redundancies and extra-normal physiologic values nature has, and engineers may, successfully addressed such anomalies.

3. Blood volume increases are necessary to address technical limitations of current tissue engineering and microfabrication techniques. A distribution-based treatment of supra-physiologic blood volumes and the example of the icefish indicate that designers have some latitude in determining HOC blood volume, especially for perfusion-limited drugs.

It is necessary to note here that increasing blood volume is not at odds with our proposal to limit oxygen supply. Since Henry's law dictates that the concentration of gas dissolved in a liquid is proportional to the partial pressure of that gas in the atmosphere and (as Fig. 2 demonstrates) cell consume oxygen in a concentration dependent manner, the overall blood volume should have little bearing on the matter in an oxygen controlled environment. If, rather than controlling the pO_2 of the culture atmosphere, a researcher sought to generate low O_2 by balancing gas exchange, consumption and flow[61], then changing blood volume may indeed necessitate a careful balance of various parameters (e.g. flow, volume, cellular O_2 consumption and media oxygen concentration).

Finally, we formalize a complete set of design parameters for a lung, liver, endothelium, fat, and heart $\times 10^{-6}$ HOC (Table 3, other tables and comparisons in Supplementary Information S5, Supplementary Tables 3–6) that follows the design principles laid out here. We further compare relevant design criteria of this more practical $\times 10^{-6}$ HOC to *C. aceratus*, a standard human, and a mouse (Fig. 6a). Values for this five-parameter comparison across blood oxygen content (blood O_2), intervessel distance (IVD), skin gas exchange, cardiac output and blood volume were drawn from many sources and normalized against values predicted by QPSRs[17,23,40,46,48,49,51,52,62–72]. For details, see Supplementary Information S6 and Supplementary Tables 7 and 8. Another set of charts predicting behavior based on these parameters is calculated and shown in (Fig. 6b), demonstrating the superiority of our holistic design strategy over an unmodified approach.

Inspired by the example of *C. aceratus* and motivated to suppress cellular BMR to physiologic levels (and to avoid the challenges inherent in developing a synthetic substitute), we have deliberately excluded Hb from this HOC design in order to restrict oxygen availability and limit cellular BMR. However, Hb also plays a key role in transporting carbon dioxide away from metabolically active tissues — carrying up to 30% of the CO_2 transported in blood[70]. In this HOC design, we justify ignoring these effects because CO_2 transport can occur by other means. At 35°C, PDMS is nearly five times more permeable to carbon dioxide than oxygen[73]. Similarly, the solubility of CO_2 and NO (nitrous oxide, an important signaling molecule) in water are both orders of magnitude greater than O_2[74–76].

Beyond oxygen transport, Hb plays important roles in other aspects of physiology including NO catalysis[70]. Depending on the specific application, each function may need to be explicitly accounted for in HOC design.

For this (or any) HOC system to be accepted as a microphysiological model of the body, some method of validating the underlying design strategy is necessary. Although directly testing such a system against humans may be challenging, we can apply the same design criteria outlined here to build rats-, mice-, etc.-on-a-chip. Parallel studies comparing the response of the microphysiological model system to the genuine animal will provide information on areas where HOCs may be particularly well- (or ill-)suited to serve as a complimentary research tool. A second approach may be to test whether an HOC is able to maintain key homeostatic parameters (e.g. blood glucose level) in the face of a reasonable challenge (e.g. bolus injection of glucose). In and of themselves, these experiments may also yield new mechanistic insights into previously unexplored aspects of common biomedical research models.

6. CONCLUSION

This work makes several key assumptions that should be verified, or at least noted, in further research. Although the section on 'Control of Cellular BMR' makes clear that we may indeed induce a more *in-vivo*-like BMR in cells by controlling the concentration of oxygen available in culture, this is not the only criterion necessary for success. Many other factors including ECM support and cell–cell interaction, and likely some yet to be discovered factors, also drive *in-vivo*-like phenotypes and must be carefully considered as part of any HOC effort. Furthermore, for the treatment of the proposed distribution-informed approach to HOC blood volume to be valid, experimentalists must know, or at least be able to suspect, the chemical properties of all drugs, metabolites and other molecules of interest within a system. To be exhaustive within a generalized experimental model, it may be necessary for researchers to use iterative processes, where a system is screened for compounds of interest then tuned accordingly and rescreened. Finally, the F-2D and F-3D classification proposed for HOC designs is likely too simplistic. While some organs fall readily into one category or the other, the truth is that most all organs behave somewhat like the liver — each has critical dependencies on *both* surface area and volume. To most accurately represent this reality, engineered, organ-specific on-chip systems would ideally represent organ compartment. However, in many cases constraints on resources and/or complexity will mean that F-2D and F-3D idealizations are sufficient in most instances.

Quarter power scaling relationships are both empirically and theoretically supported and provide guidance for sizing physiologic parameters in the face of changing system size. Their application to the development of microphysiological models of the body or "HOCs" however introduces both fundamental and technical challenges which currently frustrate efforts at design and construction of a relevant, feasible system. We posit that HOC designers may avoid these issues by selecting parameters outside the realm of what is considered physiologic so long as the ultimate function of the system is preserved. Since cell behavior is context dependent, suppressing cellular BMR on-chip to mimic *in-vivo* levels is crucial to designing a physiologically relevant HOC. We observe O_2-dependent decreases in

cell metabolism across four different cell types to demonstrate the feasibility of this approach. We use a natural experiment, the icefish, to conceptually justify this approach and demonstrate how extra-physiologic parameters may interact to give a normal physiologic response. Further study of an HOC system through a distribution-informed treatment of blood concentration of small-molecule drugs indicates that we may indeed increase HOC blood volumes with only minor consequences. In cases where even that is unacceptable, we provide frameworks to estimate the magnitude of and/or mitigate the error. Integrating these lessons in the design of a liver–lung–heart–fat–blood system, we propose a complete set of design parameters for a $\times 10^{-6}$ miniaturized HOC system. This work forms a basis of a nature-inspired approach to govern the design of *in-vitro* model systems.

7. METHODS

7.1 Oxygen conformance and cellular BMR suppression

All cell lines were obtained from ATCC and cultured in Dulbecco's Modified Eagle Medium (DMEM) supplemented with 10% Fetal Bovine Serum (FBS) and 1% antibiotic/antimycotic (anti/anti). The day before the experiment, cells were seeded in 96-well plates at 25,000 cells/well and allowed to adhere overnight. OxyCycler atmosphere control chambers (BioSphyrix, New York) were set to 2% and 7% oxygen, both with 5% CO_2. The day of the experiment, media was changed to DMEM and anti/anti without FBS and one plate was placed in each oxycycler chamber, as well as a third plate in a standard cell culture incubator (20% O_2 and 5% CO_2) and allowed to equilibrate for four hours. At that point, the media was changed again and replaced with DMEM, anti/anti and AlamarBlue metabolic indicator (Invitrogen). After a two-hour incubation, the level of reduced AlamarBlue was measured using a fluorescent plate reader (BioTek Synergy Neo) at 560/590 nm (excitation/emission).

AlamarBlue indicates cell metabolic activity by serving as an oxidizing agent during aerobic respiration, competing with oxygen for electrons at the end of the electron transport chain[70,77]. Changing oxygen levels, therefore, affect the frequency at which AlamarBlue is reduced and therefore the levels of fluorescence observed across each cell culture plate at the end of the experiment. To correct for this effect, we use Equation (7) to estimate cellular metabolic activity in the face of changing oxygen level:

$$Cellular\ BMR = AB_{Red} \cdot \frac{\Delta P_{AB} + X \cdot \Delta P_{O2}}{\Delta P_{AB}}, \quad (7)$$

where *Cellular BMR* is the corrected, unitless cellular metabolic rate measured by AlamarBlue, AB_{Red} is the fluorescent measurement from the assay, P_{AB} is the difference in reduction potential between AlamarBlue and cytochrome C, the ultimate reducing agent of oxygen in aerobic respiration, X is the fractional reduction of oxygen tension compared to a 20% O_2 atmosphere (typical for a laboratory cell culture incubator) and P_{O2} is the difference in reduction potential between O_2 and cytochrome C. Using standard values to calculate P[77], we can generate a corrected cellular BMR. We may use this unitless metric to compare relative cellular BMRs and to demonstrate the effect of oxygen tension on cellular metabolic activity. Two caveats must apply to this analysis, however. First, the

cellular BMR values compared here are *aerobic* only; we make no effort to measure energy derived from fermentation. As respiration is an order of magnitude more efficient, any error introduced by this approach is likely to be sufficiently small. Second, while these cellular BMRs are purely *relative* measurements, one may theoretically use a series of calibration experiments to arrive at a set of *absolute* measurements for cellular metabolic rates.

7.2 Distribution-informed approach to HOC blood volumes

To test the theoretical predictions of Equation (6) regarding the behavior of small-molecule drugs in the face of changing blood volumes, we constructed a crude, $\times 10^{-5}$ "pharmacokinetics-in-a-tube" system. A glass vial containing 280 μL of 1-octanol (Sigma) was used to model the tissue volume of a $\times 10^{-5}$ human and 360 μL of pH 7.4 phosphate-buffered saline (PBS, Life Technologies) represented the non-blood body water volume[55,56]. A variable amount of PBS was used to represent Z = 1, 2, 5, 10, 30, 50 and 100 conditions, where Z = 1 corresponded to a blood volume of 60 μL. The relevant drug was added to the vial, agitated, and allowed to equilibrate for ~two hours in a 5% CO_2 incubator at 37°C. After ~two hours, the organic and aqueous phases were well separated and the appropriate phase was sampled and analyzed. Each condition was performed in triplicate. For epinephrine (Sigma), a total dose of 100 μg/vial was used and the lower (aqueous) phase was sampled. Epinephrine levels were detected by an Acquity UPLC system (Waters) with a reverse-phase C18 column (Waters) and a UV-vis detector measuring absorbance at 210 nm. The mobile phase was 99% 20 mM NaH_2PO_4 at pH 2.5 and 1% MeOH. For propranolol, a total dose of 1 mg/vial was used and the aqueous phase was sampled. Propranolol (Sigma) levels were detected on a Synergy plate reader (BioTek) by reading fluorescence at 289/353 nm. For amiodarone (Sigma), the total dose/vial was 0.56 mg and the upper (organic) phase was sampled. Amiodarone levels were detected by fluorescence at 388/475 nm.

To investigate the implications of changing organic phase mass on a living system, we used a liver-adipospheroid co-culture platform. 3T3-L1 preadipocytes were expanded and differentiated into adipose tissues in 3D spheroid culture as described previously with 8,000 cells per spheroid[24]. HepG2-C3A liver cells were seeded in a clear bottom, black-wall 96-well plate (Corning Costar) at a density of 10,000 cells/well and given six hours to attach. After adipose spheroid differentiation, the spheroids were collected from the hanging drop plate and added to the 2D liver cell culture (0, 4 or 12 per well) in 30 μL of media volume. Amiodarone (dissolved in DMSO) and acetaminophen were then added to the culture wells and incubated for 24 hours. After the incubation period, media and spheroids were aspirated and the HepG2-C3A monolayer was washed once gently and AlamarBlue indicator was added. HepG2 viability was measured by taking a fluorescence reading at 560/590 (ex/em) after two hours. Data was analyzed using two-way ANOVA with Tukey's post-test.

Supplementary Material

Refer to Web version on PubMed Central for supplementary material.

Acknowledgments

References

1. Huh D, et al. Reconstituting organ-level lung functions on a chip. Science. 2010; 328(5986):1662–1668. [PubMed: 20576885]

2. Moraes C, Mehta G, Lesher-Perez SC, Takayama S. Organs-on-a-chip: A focus on compartmentalized microdevices. Ann Biomed Eng. 2012; 40(6):1211–1227. [PubMed: 22065201]

3. Bhatia SN, Ingber DE. Microfluidic organs-on-chips. Nat Biotechnol. 2014; 32(8):760–772. [PubMed: 25093883]

4. Sung JH, et al. Microfabricated mammalian organ systems and their integration into models of whole animals and humans. Lab Chip. 2013; 13(7):1201. [PubMed: 23388858]

5. Sung JH, Kam C, Shuler ML. A microfluidic device for a pharmacokinetic–pharmacodynamic (PK–PD) model on a chip. Lab Chip. 2010; 10(4):446. [PubMed: 20126684]

6. Vozzi F, Heinrich JM, Bader A, Ahluwalia AD. Connected culture of murine hepatocytes and human umbilical vein endothelial cells in a multicompartmental bioreactor. Tissue Eng Part A. 2008; 15(6):1291–1299.

7. Maschmeyer I, et al. A four-organ-chip for interconnected long-term co-culture of human intestine, liver, skin and kidney equivalents. Lab Chip. 2015; 15(12):2688–2699. [PubMed: 25996126]

8. Esch MB, et al. How multi-organ microdevices can help foster drug development. Adv Drug Deliv Rev. 2014; 69–70:158–169.

9. National Center for Advancing Translational Sciences (NCATS). Tissue chip for drug screening. 2012. ncats.nih.gov/tissue-chip.html

10. Polini A, et al. Organs-on-a-chip: A new tool for drug discovery. Expert Opin Drug Discov. 2014; 9(4):335–352. [PubMed: 24620821]

11. Kleiber M. Body size and metabolic rate. Physiol Rev. 1947; 27(4):511–541. [PubMed: 20267758]

12. White CR. Allometric scaling of mammalian metabolism. J Exp Biol. 2005; 208(9):1611–1619. [PubMed: 15855392]

13. West GB, Brown JH, Enquist BJ. A general model for the origin of allometric scaling laws in biology. Science. 1997; 276(5309):122–126. [PubMed: 9082983]

14. Banavar JR, et al. A general basis for quarter-power scaling in animals. Proc Natl Acad Sci USA. 2010; 107(36):15816–15820. [PubMed: 20724663]

15. Iori E, et al. Glucose and fatty acid metabolism in a 3 tissue *in-vitro* model challenged with normo- and hyperglycaemia. PLoS ONE. 2012; 7(4):e34704. [PubMed: 22509346]

16. Mazzei D, Guzzardi MA, Giusti S, Ahluwalia A. A low shear stress modular bioreactor for connected cell culture under high flow rates. Biotechnol Bioeng. 2010; 106(1):127–137. [PubMed: 20091740]

17. Mattei G, Giusti S, Ahluwalia A. Design criteria for generating physiologically relevant *in-vitro* models in bioreactors. Processes. 2014; 2(3):548–569.

18. Marx U, et al. "Human-on-a-chip" developments: A translational cutting-edge alternative to systemic safety assessment and efficiency evaluation of substances in laboratory animals and man? Altern Lab Anim-ATLA. 2012; 40(5):235.

19. Viravaidya K, Sin A, Shuler ML. Development of a microscale cell culture analog to probe naphthalene toxicity. Biotechnol Prog. 2004; 20(1):316–323. [PubMed: 14763858]

20. Esch MB, Mahler GJ, Stokol T, Shuler ML. Body-on-a-chip simulation with gastrointestinal tract and liver tissues suggests that ingested nanoparticles have the potential to cause liver injury. Lab Chip. 2014; 14(16):3081. [PubMed: 24970651]

21. Abaci HE, Shuler M. Human-on-a-chip design strategies and principles for physiologically based pharmacokinetics/pharmacodynamics modeling. Integr Biol. 2015; 7(4):383–391.

22. Wikswo JP, et al. Engineering challenges for instrumenting and controlling integrated organ-on-chip systems. IEEE Trans Biomed Eng. 2013; 60(3):682–690. [PubMed: 23380852]

23. Wikswo JP, et al. Scaling and systems biology for integrating multiple organs-on-a-chip. Lab Chip. 2013; 13(18):3496. [PubMed: 23828456]

24. Moraes C, et al. On being the right size: Scaling effects in designing a human-on-a-chip. Integr Biol. 2013; 5(9):1149.

25. West GB, Woodruff WH, Brown JH. Allometric scaling of metabolic rate from molecules and mitochondria to cells and mammals. Proc Natl Acad Sci U S A. 2002; 99(Suppl. 1):2473–2478. [PubMed: 11875197]

26. Porter RK, Brand MD. Cellular oxygen consumption depends on body mass. Am J Physiol-Regul Integr Comp Physiol. 1995; 269(1):R226–R228.

27. Brown MF, Gratton TP, Stuart JA. Metabolic rate does not scale with body mass in cultured mammalian cells. Am J Physiol Regul Integr Comp Physiol. 2007; 292(6):R2115–R2121. [PubMed: 17234960]

28. Heusner AA. Size and power in mammals. J Exp Biol. 1991; 160(1):25–54. [PubMed: 1960515]

29. Wang W, Upshaw L, Strong DM, Robertson RP, Reems J. Increased oxygen consumption rates in response to high glucose detected by a novel oxygen biosensor system in non-human primate and human islets. J Endocrinol. 2005; 185(3):445–455. [PubMed: 15930171]

30. Wataha JC, Hanks CT, Craig RG. *In-vitro* effect of metal ions on cellular metabolism and the correlation between these effects and the uptake of the ions. J Biomed Mater Res. 1994; 28(4): 427–433. [PubMed: 8006047]

31. Huang G, Greenspan DS. ECM roles in the function of metabolic tissues. Trends Endocrinol Metab. 2012; 23(1):16–22. [PubMed: 22070921]

32. Mehta G, et al. Quantitative measurement and control of oxygen levels in microfluidic poly(dimethylsiloxane) bioreactors during cell culture. Biomed Microdevices. 2007; 9(2):123–134. [PubMed: 17160707]

33. Lo JF, Sinkala E, Eddington DT. Oxygen gradients for open well cellular cultures via microfluidic substrates. Lab Chip. 2010; 10(18):2394. [PubMed: 20559583]

34. Oppegard SC, Nam KH, Carr JR, Skaalure SC, Eddington DT. Modulating temporal and spatial oxygenation over adherent cellular cultures. PLoS ONE. 2009; 4(9):e6891. [PubMed: 19727397]

35. Schumacker PT, Chandel N, Agusti AG. Oxygen conformance of cellular respiration in hepatocytes. Am J Physiol Lung Cell Mol Physiol. 1993; 265(4):L395–L402.

36. Ahluwalia A. Allometric scaling *in-vitro*. Sci Rep. 2017; 7:42113. [PubMed: 28169362]

37. Wikswo JP. The relevance and potential roles of microphysiological systems in biology and medicine. Exp Biol Med. 2014; 239(9):1061–1072.

38. Gon, O., Heemstra, PC. Fishes of the Southern Ocean. J.L.B. Smith Institute of Icdhthyology; South Africa: 1990.

39. Regan CT. II. The Antarctic fishes of the Scottish National Antarctic expedition. Trans R Soc Edinb. 1913; 49(02):229–292.

40. Ruud JT. Vertebrates without erythrocytes and blood pigment. Nature. 1954; 173(4410):848–850. [PubMed: 13165664]

41. Hemmingsen, EA. Respiratory and cardiovascular adaptations in hemoglobin-free fish: Resolved and unresolved problems. In: di Prisco, G.Maresca, B., Tota, B., editors. Biology of Antarctic Fish. Springer; 1991. p. 191-203.

42. Sidell BD, O'Brien KM. When bad things happen to good fish: The loss of hemoglobin and myoglobin expression in Antarctic icefishes. J Exp Biol. 2006; 209(10):1791–1802. [PubMed: 16651546]

43. FishBase. Notothenia coriiceps. 2005. http://www.fishbase.se/Photos/PicturesSummary.php?ID=4702&what=species

44. Ralph R, Everson I. The respiratory metabolism of some Antarctic fish. Comp Biochem Physiol. 1968; 27:299–307.

45. Holeton GF. Oxygen uptake and circulation by a hemoglobinless Antarctic fish (*Chaenocephalus aceratus* Lonnberg) compared with three red-blooded Antartic fish. Comp Biochem Physiol. 1970; 34(2):457–471. [PubMed: 5426570]

46. Hemmingsen EA, Douglas EL. Respiratory characteristics of the hemoglobin-free fish *Chaenocephalus aceratus*. Comp Biochem Physiol. 1970; 33(4):733–744. [PubMed: 5421990]

47. Egginton S. Blood rheology of Antarctic fishes: Viscosity adaptations at very low temperatures. J Fish Biol. 1996; 48(3):513–521.

48. Hemmingsen EA, Douglas EL, Johansen K, Millard RW. Aortic blood flow and cardiac output in the hemoglobin-free fish *Chaenocephalus aceratus*. Comp Biochem Physiol A Physiol. 1972; 43(4):1045–1051.

49. Acierno R, MacDonald JA, Agnisola C, Tota B. Blood volume in the hemoglobin-less Antarctic teleost *Chionodraco hamatus* (Lönnberg). J Exp Zool. 1995; 272(5):407–409.

50. Eastman, JT. Antarctic Fish Biology: Evolution in a Unique Environment. Academic Press Limited; 1993.

51. Twelves EL. Blood volumes of two Antarctic fishes. Antarct Surv Bull. 1972; 31:85–92.

52. Wujcik JM, Wang G, Eastman JT, Sidell BD. Morphometry of retinal vasculature in Antarctic fishes is dependent upon the level of hemoglobin in circulation. J Exp Biol. 2007; 210(5):815–824. [PubMed: 17297141]

53. Bianconi E, et al. An estimation of the number of cells in the human body. Ann Hum Biol. 2013; 40(6):463–471. [PubMed: 23829164]

54. Allen JW, Bhatia SN. Formation of steady-state oxygen gradients *in-vitro*: Application to liver zonation. Biotechnol Bioeng. 2003; 82(3):253–262. [PubMed: 12599251]

55. Shargel, L., Yu, ABC. Applied Biopharmaceutics and Pharmacokinetics. Appleton & Lange; 1993.

56. Rowland, M., Tozer, TN. Clinical Pharmacokinetics: Concepts and Applications. Williams & Wilkins; 1995.

57. Sbrana T, Ahluwalia A. Engineering Quasi-Vivo® *in-vitro* organ models. Adv Exp Med Biol. 2012; 745:138–153. [PubMed: 22437817]

58. Wolinsky H. A proposal linking clearance of circulating lipoproteins to tissue metabolic activity as a basis for understanding atherogenesis. Circ Res. 1980; 47(3):301–311. [PubMed: 6996862]

59. Jaffe EA. Cell biology of endothelial cells. Hum Pathol. 1987; 18(3):234–239. [PubMed: 3546072]

60. Augustin HG, Kozian DH, Johnson RC. Differentiation of endothelial cells: Analysis of the constitutive and activated endothelial cell phenotypes. BioEssays. 1994; 16(2):901–906. [PubMed: 7840769]

61. Mehta G, et al. Hard top soft bottom microfluidic devices for cell culture and chemical analysis. Anal Chem. 2009; 81(10):3714–3722. [PubMed: 19382754]

62. Petschow R, Petschow D, Bartels R, Baumann R, Bartels H. Regulation of oxygen affinity in blood of fetal, newborn and adult mouse. Respir Physiol. 1978; 35(3):271–282. [PubMed: 33429]

63. Williams LR, Leggett RW. Reference values for resting blood flow to organs of man. Clin Phys Physiol Meas. 1989; 10(3):187. [PubMed: 2697487]

64. Egginton S. Control of tissue blood flow at very low temperatures. J Therm Biol. 1997; 22(6):403–407.

65. Tournoux F, et al. Validation of noninvasive measurements of cardiac output in mice using echocardiography. J Am Soc Echocardiogr. 2011; 24(4):465–470. [PubMed: 21315557]

66. Stücker M, et al. The cutaneous uptake of atmospheric oxygen contributes significantly to the oxygen supply of human dermis and epidermis. J Physiol. 2002; 538(3):985–994. [PubMed: 11826181]

67. Brandrup, J., Immergut, EH., Grulke, EA. Polymer Handbook. John Wiley & Sons; 1998.

68. Folarin AA, Konerding MA, Timonen J, Nagl S, Pedley RB. Three-dimensional analysis of tumour vascular corrosion casts using stereoimaging and micro-computed tomography. Microvasc Res. 2010; 80(1):89–98. [PubMed: 20303995]

69. Malkusch W, Konerding MA, Klapthor B, Bruch J. A simple and accurate method for 3-D measurements in microcorrosion casts illustrated with tumour vascularization. Anal Cell Pathol. 1995; 9(1):69–81. [PubMed: 7577757]

70. Widmaier, EP., Raff, H., Strang, KT. Vander's Human Physiology. McGraw-Hill; 2006.

71. Peters, RH. The Ecological Implications of Body Size. Cambridge University Press; 1983.

72. Schmidt-Nielsen, K. Scaling: Why Is Animal Size So Important?. Cambridge University Press; 1984.

73. Merkel TC, Bondar VI, Nagai K, Freeman BD, Pinnau I. Gas sorption, diffusion, and permeation in poly (dimethylsiloxane). J Polym Sci B Polym Phys. 2000; 38(3):415–434.

74. Weiss RF. The solubility of nitrogen, oxygen and argon in water and seawater. Deep Sea Res Oceanogr Abstr. 1970; 17(4):721–735.

75. Weiss RF. Carbon dioxide in water and seawater: The solubility of a non-ideal gas. Mar Chem. 1974; 2:203–215.

76. Weiss RF, Price BA. Nitrous oxide solubility in water and seawater. Mar Chem. 1980; 8:347–359.

77. Invitrogen. AlamarBlue Technical Datasheet. https://tools.thermofisher.com/content/sfs/manuals/PI-DAL1025-1100_TI%20alamarBlue%20Rev%201.1.pdf
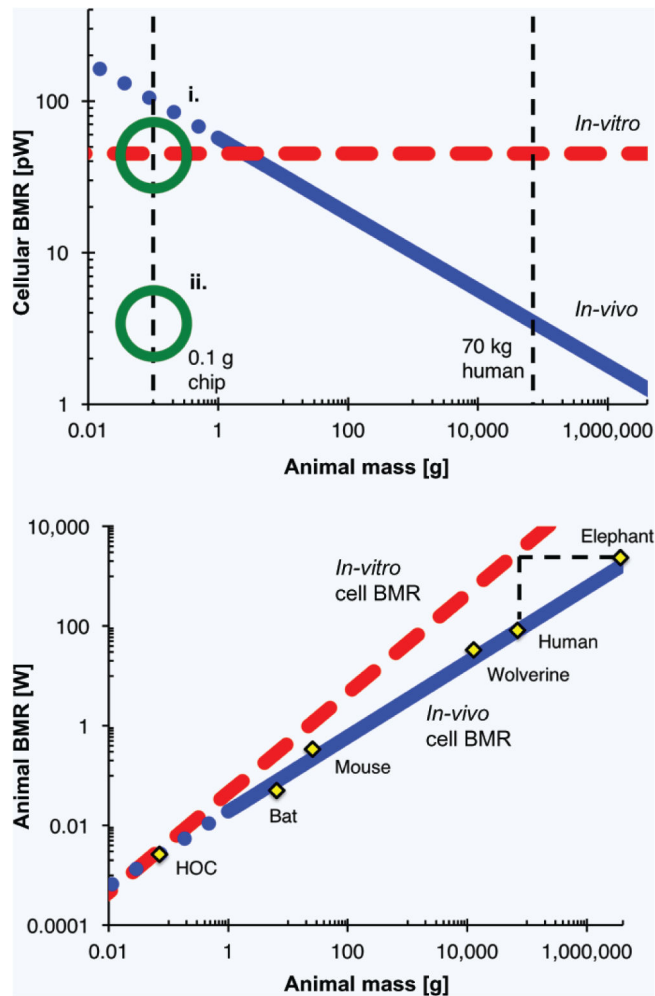
Figure 1.

Consequences of context-dependent cellular basal metabolic rate (BMR). (**a**) Cellular BMR scales as $\propto M^{-\frac{1}{4}}$ *in-vivo* but mammalian cells cultured *in-vitro* have the same cellular BMR regardless of the mass of the source organism ($\propto M^{0}$). (**a–i**) *In-vitro* cell culture of human cells leads to a cellular BMR ~one order of magnitude larger than that of a normal human[25,27]. (**a–ii**) A high-fidelity, physiologically relevant human-on-a-chip (HOC) should be designed with mechanisms to ensure cellular BMR matches typical *in-vivo* values for the organism to be modeled. (**b**) Failure to account for the context-dependent behavior of cells can substantially alter the modeled system BMR, especially for larger animals[25,28]. Graphs reproduced using previously published data and relationships[25,28,72].
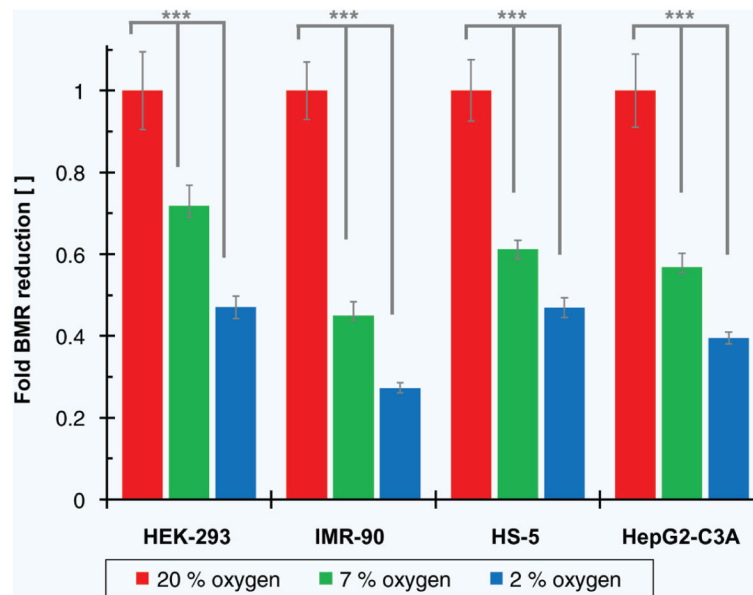
Figure 2.
AlamarBlue metabolic indicator was used to measure cellular BMR in different oxygen tension environments. Correcting for the effect of oxygen on AlamarBlue fluorescence, we observed a marked decrease in respiration with falling oxygen levels across four different cell lines. A 10-fold reduction in oxygen reduced cellular respiration by a factor of nearly five. Data plotted as average ± standard deviation for $n = 7$. *** indicates $p < 0.001$ by one-way ANOVA with Tukey post-test.
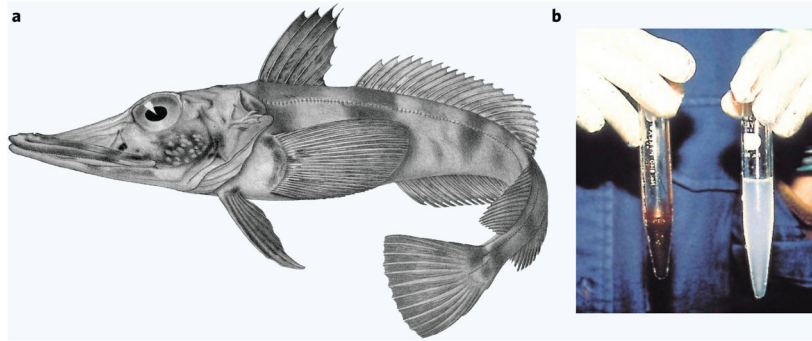
Figure 3.
(**a**) Artist's rendering of *C. aceratus*, a hemoglobin-free fish living in the Southern Ocean near Antarctica. Used with permission of Regan[39]. (**b**) Freshly drawn blood from *C. aceratus* (right) is milky white while blood from Hb+ *N. coriiceps* is a familiar shade of red (left). Adapted with permission from Sidell & O'Brien[42].
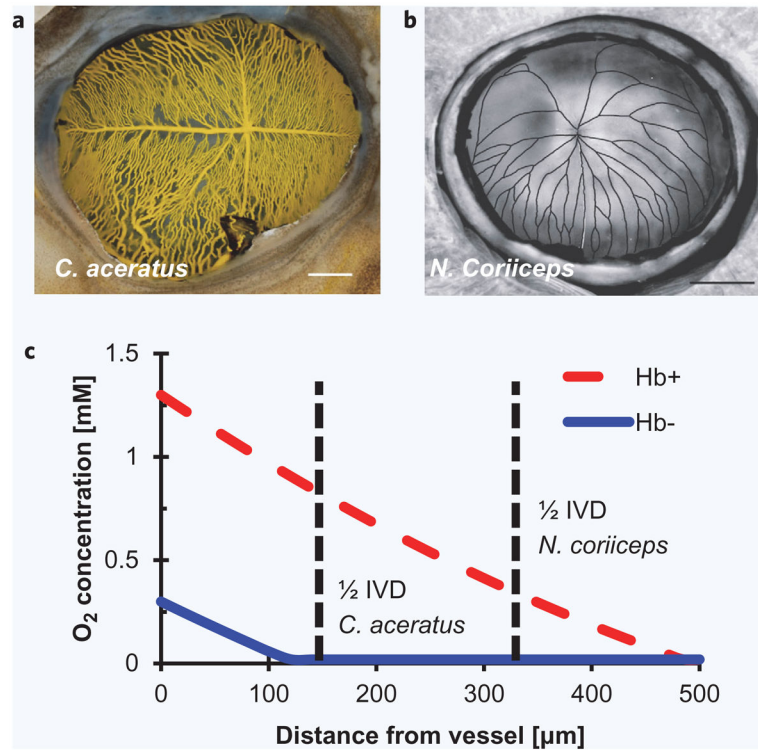
Figure 4.

O$_2$ delivery in *Nototenioidei*. Retinal micrographs of (**a**) *C. aceratus* (**b**) *N. co riiceps* demonstrate the difference in capillary density and intervessel distance (IVD) between the two fish. Reprinted with permission from Wujcik *et al.*[52]. (**c**) These decreased intervessel distances help compensate for blood O$_2$ levels in *C. aceratus*. A similar effect should act on other solute (e. growth factors or drugs) diluted by larger blood volumes as well. Equation (1) solved numerically using MatLab and data from Refs. 17, 40, 52 and 53; full list of parameter values can be found in Supplementary Information S1.4.
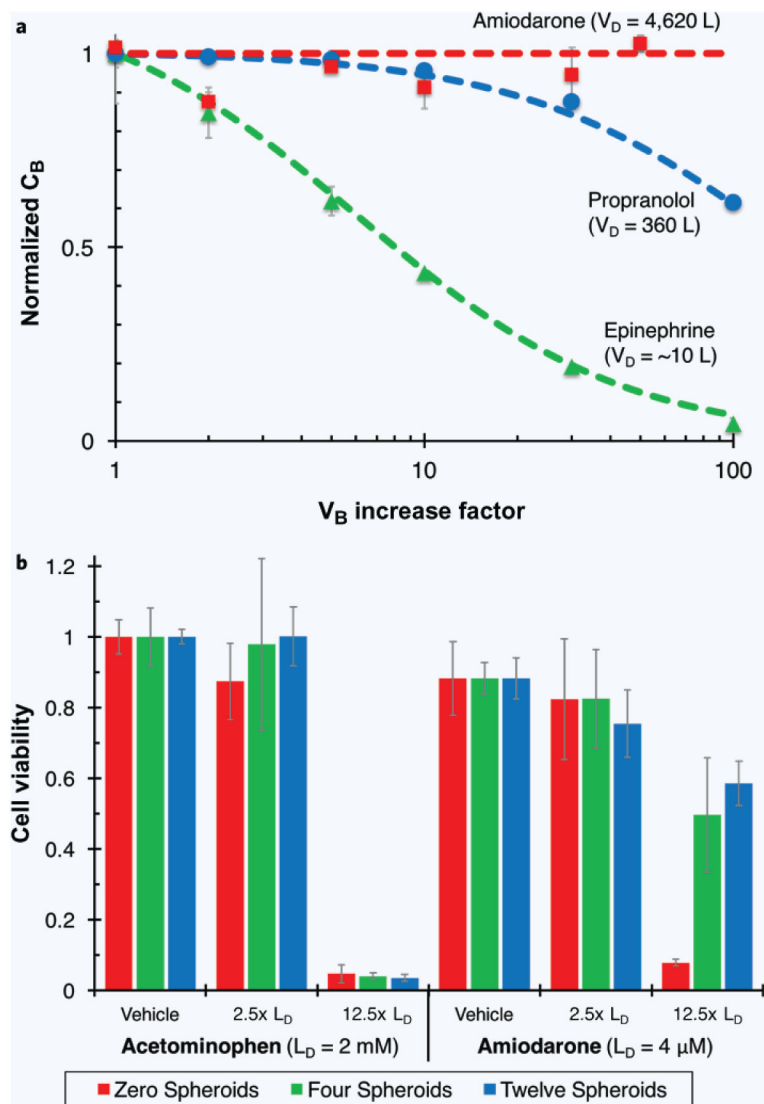
Figure 5.
Altering aqueous to organic volume proportions affects concentration and toxicity of various drugs. (**a**) Increased blood volumes minimally effect blood concentration depending on drug properties for perfusion-limited drugs according to Equation (6). Hydrophobic drugs (e.g. amiodarone) partition mostly to tissue and blood concentration is largely unaffected by changes in blood volume. More hydrophilic drugs (e.g. epinephrine) partition largely to the blood and are more affected by large changes in blood volume. (**b**) In a live-cell experiment, increasing mass of the organic phase (i.e. addition of more adipospheroids) rescues HepG2-C3A liver cells from toxicity of a hydrophobic drug (Amiodarone, lethal dose 4 μM), but not a hydrophilic drug (acetaminophen, lethal dose 2 mM). Data plotted as average ± S.D. for n = 7.

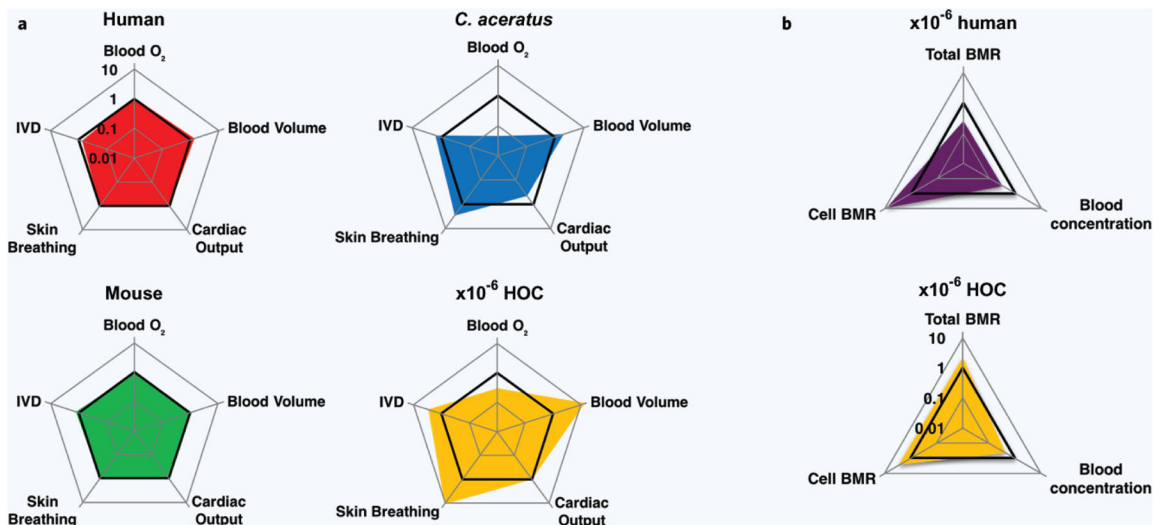*** indicates $p < 0.001$ by two-way ANOVA with Tukey post-test.

Figure 6.

Design and performance of natural and artificial physiological systems. (**a**) Radar charts comparing *design* parameter values for a human, a mouse, the Hb− icefish *C. Aceratus*, and a ×10⁻⁶ miniaturized HOC. Values plotted on a log scale and normalized to QPSR estimates for all graphs. Note that observed values for the mouse and human match QPSR estimates (bold lines) closely while the general shape of the charts for *C. Aceratus* and the HOC have similar shapes. A ×10⁻⁶ human designed only according to QPSRs would lie exactly along the bolded line representing a normalized value of 1. Without additional controls, this ×10⁻⁶ model would have abnormally high per cell and system metabolism. (**b**) Applying the modifications proposed here to build a ×10⁻⁶ HOC is predicted to lead to a more accurate model of the human body measured across three key *functional* parameters. Compared to an QPSR-scaled ×10⁻⁶ human with a minimum blood volume limited by technical challenges (top) and despite straying from conventional parameters, our design strategy yields a ×10⁻⁶ HOC (bottom) that more closely matches human levels of cellular BMR, system BMR and blood concentration of a low volume distribution drug (e.g. epinephrine). Computed using data from Refs. 17, 23, 40, 46, 48, 49, 51, 52, 62–72.

Table 1

Physiological values for a hypothetical 1 kg test-fish as hemoglobin (Hb) is removed and icefish characteristics introduced.

Condition imposed on the test-fish	O$_2$ solubility in blood [mg/mL][*]	Cardiac output (Q) [mL/h]	Cutaneous respiration [mg O$_2$/h]	Maximum O$_2$ delivery [mg/h]
Normal	0.085[40]	3,900[64]	—	330
–Hb	0.0095[40]	3,900[64]	—	37
–Hb, ↑Q	0.0095[40]	7,140[48]	—	68
–Hb, ↑Q, +C. Resp.	0.0095[40]	7,140[48]	10[41]	78
	N. coriiceps resting VO$_2$ = 42 mg O$_2$/h[45,46]			
	C. aceratus resting VO$_2$ = 32 mg O$_2$/h[44–46]			

[*]Measured at 0°C and 101.3 kPa.

Table 2

Design strategy for different HOC organ compartment classes defined by metabolically supported functional scaling (MSFS) theory.

HOC organ compartment class	Tissue size	Blood volume
F-2D	Surface area constrained, $\propto M^1$ scaling from macro human	Dimensions selected to maintain physiologic shear given fractional cardiac output
F-3D	Volume constrained, $\propto M^1$ scaling from macro human	Calculated so that organ blood volume matches target fractional organ mass of whole body
F-2.5D	Divided into F-2D and F-3D domains with each domain scaled per F-2D or F-3D design rules	

Table 3

A comprehensive table of design parameters for a five-organ $\times 10^{-6}$ HOC. We propose increasing blood volume levels beyond those called for by conventional quarter-power scaling relationships (QPSRs) to account for engineering limitations in organ design. Chamber dimensions are selected to match *in-vivo* shear levels (F-2D) or match *in-vivo* mass (F-3D).

Organ		Class	Surface area [mm²]	Tissue mass [mg]	Blood volume (BV) [µL]	% BV	% CO	Compartment dimension		
								Length [mm]	Width [mm]	Height [mm]
Lung	Endothelium	F-2D	30	0.12	1.1	—	—	—	—	—
	Non-EC	F-2D	40	0.16	1.4	—	—	—	—	—
	Total	F-2D	70	0.28	2.5	4	100	9.02	7.76	0.035
Liver	Endothelium	F-2D	80	0.32	2	—	—	14.87	5.38	0.025
	Non-EC	F-3D	34	1.75	1.03	—	—	1.57	1.57	1
	Total	F-2/3D	114	2.07	3.03	5	25	—	—	—
Heart		F-3D	—	0.33	0.28	0.5	4	1.06	1.06	0.5
Fat		F-3D	—	12.5	10.7	18	5	4.96	4.96	1
Blood		—	—	—	60	—	—	—	—	—
"Other Tissues"		F-3D	—	48.8	43.5	73	66	6.6	6.6	1
Blood Oxygen Content [BL-O2; mM]					~2					
Cutaneous Respiration [mol/m/s/mmHg]					3.8×10^{-11}					
Cardiac Output [mL/s]					3.4×10^{-3}					
Intervessel Distance [IVD; µm]					250					